LUND UNIVERSITY

Waveguide modes for current approximation in frequency selective surfaces

Poulsen, Sören

2006

Link to publication

Citation for published version (APA):
Poulsen, S. (2006). *Waveguide modes for current approximation in frequency selective surfaces.* (Technical Report LUTEDX/(TEAT-7147)/1-10/(2006); Vol. TEAT-7147). [Publisher information missing].

Total number of authors:
1

General rights
Unless other specific re-use rights are stated the following general rights apply:
Copyright and moral rights for the publications made accessible in the public portal are retained by the authors and/or other copyright owners and it is a condition of accessing publications that users recognise and abide by the legal requirements associated with these rights.
• Users may download and print one copy of any publication from the public portal for the purpose of private study or research.
• You may not further distribute the material or use it for any profit-making activity or commercial gain
• You may freely distribute the URL identifying the publication in the public portal

Read more about Creative commons licenses: https://creativecommons.org/licenses/

Take down policy
If you believe that this document breaches copyright please contact us providing details, and we will remove access to the work immediately and investigate your claim.

LUND UNIVERSITY

PO Box 117
221 00 Lund
+46 46-222 00 00

Download date: 18. Dec. 2025

CODEN:LUTEDX/(TEAT-7147)/1-10/(2006)

Waveguide modes for current approximation in frequency selective surfaces

Sören Poulsen

Electromagnetic Theory
Department of Electrical and Information Technology
Lund University
Sweden

(TEAT-7147)/1-10/(2006): S. Poulsen, Waveguide modes for current approximation in frequency selective surfaces

Sören Poulsen

Department of Electrical and Information Technology
Electromagnetic Theory
Lund University
P.O. Box 118
SE-221 00 Lund
Sweden

Editor: Gerhard Kristensson
© Sören Poulsen, Lund, August 28, 2006

CODEN:LUTEDX/(TEAT-7147)/1-10/(2006)

Waveguide modes for current approximation in frequency selective surfaces

Sören Poulsen

Electromagnetic Theory
Department of Electrical and Information Technology
Lund University
Sweden

Sören Poulsen

Department of Electrical and Information Technology
Electromagnetic Theory
Lund University
P.O. Box 118
SE-221 00 Lund
Sweden

Editor: Gerhard Kristensson
© Sören Poulsen, Lund, August 28, 2006

Abstract

The importance of using efficient bases for current expansion in numerical computations of electromagnetic field problems has been emphasized for several decades. It is well known that the basis functions should approximate the physical current (electric or magnetic) to some extent. Moreover, for efficiency, it is reasonably to require that only a few basis functions are needed in order to obtain adequate results. Bases for specific frequency selective surface (FSS) element geometries has frequently been suggested, however, few papers address general element geometries. In this paper we establish an efficient set of basis functions, for a general element geometry, with the finite element method (FEM). The Helmholtz' eigenvalue problem is solved by the FEM in order to obtain the waveguide modes of a waveguide with the same cross section as the considered FSS element. The transverse electric field of the first n waveguide modes, ordered by the size of the corresponding eigenvalues, are used for current approximation (electric or magnetic) in the method of moment (MoM) analysis of the FSS. These current modes are Fourier transformed by FFT using the zero-padding technique. Generally, it is found that only a few waveguide modes, typically 10, are required in order to obtain adequate results. It is also found that obtained results agrees very well with results obtained by Periodic Moment Method (PMM) code.

1 Introduction

Basis functions for specific frequency selective surface (FSS) element geometries, for instance the tripole element [16], the ring element [8] and the square loop element [3], has sporadically been suggested over time. However, few papers address general element geometries. One category of general approaches, which sometimes is referred to as the pixel approach, is based on subdomain basis functions. Subdomain bases, for instance rooftop basis functions [13] or RWG bases [12], can easily be adapted to complex element geometries. However, generally speaking, the main drawback of subdomain bases is that the double infinite Floquet mode sum corresponding to subdomain basis functions converge very slowly, due to the small support of the subdomain basis functions, since the small support in turn implies that the Fourier transform of the basis function decays slowly. Another drawback of subdomain bases is that the number of unknown current coefficients tends to be large.

An efficient general approach for the analysis of arbitrary shaped FSS elements is developed at the Ohio State University [1, 6]. Although this approach is very efficient, it uses current modes which have support on wires, rather than on flat, infinitely thin elements as treated here.

A third general approach uses so called V-dipole basis functions [11] which can be applied to centre connected and loop type elements consisting of straight segments and rounded corners. The present approach does not obey to this limitations, since it can handle a wide range of element geometries.

In the next section, we derive the waveguide modes, which then in the following section are used for current approximation in several FSS configurations. The

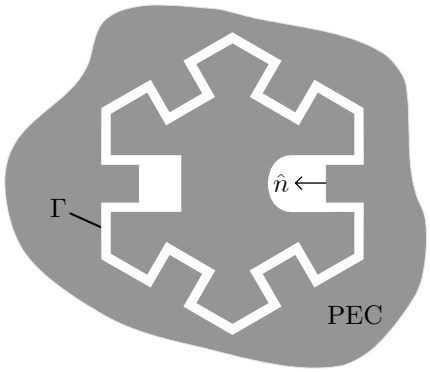

Figure 1: An example of a complex FSS element geometry.

current modes are Fourier transformed by FFT using the zero-padding technique. The obtained results are compared with the Periodic Method of Moment (PMM) code [2] as well as with the Oresme FSS code [11].

2 Methods

2.1 Waveguide modes

In order to obtain waveguide modes useful for current expansion, we consider a homogeneous closed waveguide with arbitrary cross section, which is uniform along the z-axis. The Ω region represents the waveguide cross section and Γ the boundary of Ω, with the associated inward directed unit normal $\hat{n}$, see Figure 1.

The waveguide modes are obtained from Helmholtz' eigenvalue problem. The TE modes fulfil the natural boundary condition (Neumann condition) on the boundary Γ as [14]

$$\begin{cases} \nabla_t^2 H_z(\boldsymbol{\rho}) + k_t^2 H_z(\boldsymbol{\rho}) = 0 & \boldsymbol{\rho} \in \Omega \\ \hat{n} \cdot \nabla H_z(\boldsymbol{\rho}) = 0 & \boldsymbol{\rho} \in \Gamma \end{cases} \tag{2.1}$$

while the TM modes fulfil the Dirichlet condition at the boundary as

$$\begin{cases} \nabla_t^2 E_z(\boldsymbol{\rho}) + k_t^2 E_z(\boldsymbol{\rho}) = 0 & \boldsymbol{\rho} \in \Omega \\ E_z(\boldsymbol{\rho}) = 0 & \boldsymbol{\rho} \in \Gamma \end{cases} \tag{2.2}$$

where $H_z(\boldsymbol{\rho})$ and $E_z(\boldsymbol{\rho})$ is the longitudinal magnetic and electric field, respectively, and where the tangential wavenumber k_t is the eigenvalue. The gradient operator transverse to the z-axis is defined as $\nabla_t = \nabla - \hat{z}\partial_z$. The transverse spatial coordinates are $\boldsymbol{\rho} = \hat{x}x + \hat{y}y$.

The eigenvalue problems (2.1) and (2.2) are solved by the FEM using the commercial code FlexPDE 3.0. A desired number of eigenfunctions $H_z(\boldsymbol{\rho})$ and $E_z(\boldsymbol{\rho})$, with corresponding eigenvalues k_t, are computed. The eigenfunctions and eigenvalues are independent of frequency. Once the eigenmodes $H_z(\boldsymbol{\rho})$ and $E_z(\boldsymbol{\rho})$ are known,

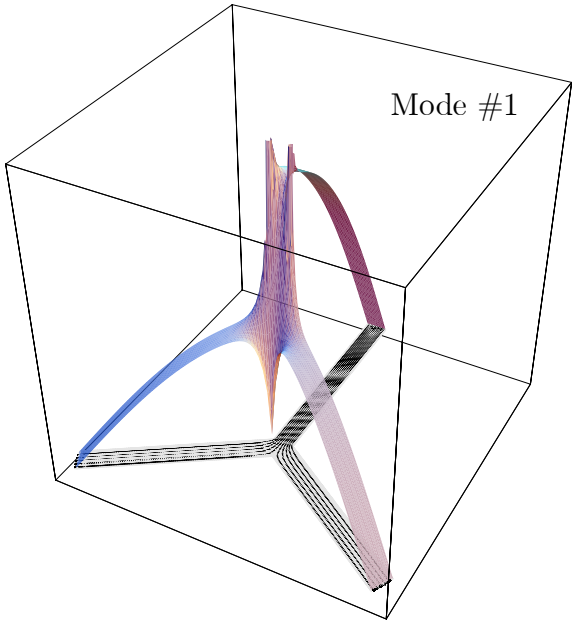

Figure 2: The amplitude of the first current mode. Notice that current lines are drawn on the surface of the element.

the transverse electric field is given as

$$\boldsymbol{E}_t(\boldsymbol{\rho}) \propto \begin{cases} \hat{z} \times \nabla_t H_z(\boldsymbol{\rho}) & \text{TE modes} \\ \nabla_t E_z(\boldsymbol{\rho}) & \text{TM modes} \end{cases}$$

where the symbol $\propto$ denotes proportional to.

2.2 Current modes

We now introduce the the magnetic current as

$$\boldsymbol{m}(\boldsymbol{\rho}) = \hat{z} \times \boldsymbol{E}_t(\boldsymbol{\rho}) \propto \begin{cases} \nabla_t H_z(\boldsymbol{\rho}) & \text{TE modes} \\ \hat{z} \times \nabla_t E_z(\boldsymbol{\rho}) & \text{TM modes} \end{cases} \tag{2.3}$$

Hence, each eigenmode has an associated magnetic current mode, given by (2.3), which is used for magnetic current expansion in slot arrays. For patch FSSes, the current modes (2.3) are used for expansion of the electric current.

Generally, for elements where the width is small compared to the length, the lowest order modes are found to be TE modes. For instance, the dominating modes of an rectangular waveguide, where the side a is considerably larger than the height b, are the TE_{m0} modes. More specifically, the number of TE_{m0} modes with lower eigenvalue than the TM_{11} mode is approximately given by $(a^2/b^2+1)^{1/2}$. The current modes corresponding to the TE_{m0} modes, which are given by $H_z(\boldsymbol{\rho}) = \cos m\pi x/a$ [4], is given by

$$\boldsymbol{m}(\boldsymbol{\rho}) \propto \hat{x} \sin m\pi x/a, \;\; m = 1, 2, \ldots \tag{2.4}$$

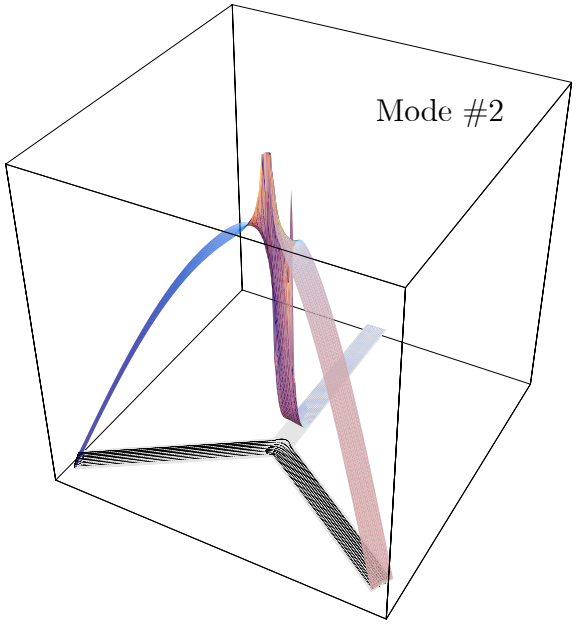

Figure 3: Mode 2 for the three legged element.

according to (2.3), where a is the length of the rectangular slot, aligned along the x-axis. Notice that these current modes are identical to them often used for thin rectangular slots and dipoles [5].

For illustration of numerical waveguide modes, obtained by the FEM, we consider the three legged element. The first three current modes are depicted in Figure 2–4. Notice that both the amplitude, *i.e.*, $|\boldsymbol{m}(\boldsymbol{\rho})|$, and the current lines of the current modes are depicted in the figures.

2.3 FFT and the method of moments

Once the current modes are obtained by the FEM, as described in Section 2.1, the scattering problem is solved by the spectral Galerkin method [15], *i.e.*, a spectral domain formulation of the method of moments. In the spectral Galerkin method the Fourier transform of the current modes is required. Hence, the numerical representation of the current modes in the spatial domain, obtained by the FEM, is transformed to the spectral domain by the fast Fourier transform (FFT). The current modes are given over a square lattice, with $N \times N$ points, in the spatial domain. In order to obtain sufficient resolution in the spectral domain, the zero-padding technique [7] is applied. When applying zero-padding, the original $N \times N$ data points are extended with a number of zeros forming a zero-padded array of the size $M \times M$, where $M \geq N$, see Figure 5. In this paper we use the `DFFT2D` IMSL subroutine to transform the zero-padded data. This subroutine is most efficient when M is a product of small prime factors. After applying FFT, the Fourier transformed data is given over a rectangular grid in the spectral domain. Intermediate values, required in the MoM procedure, are obtained by interpolation in two dimensions.

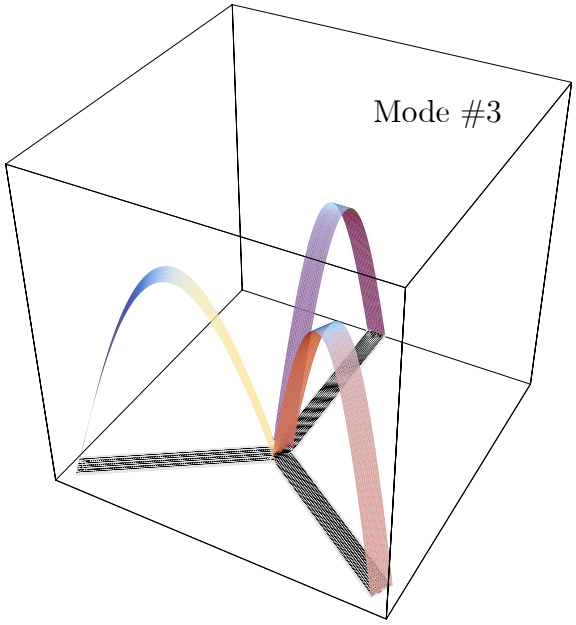

Figure 4: Mode 3 for the three legged element.

The Fourier transform of the current modes can also be calculated by numerical integration in two dimensions. Although numerical integration is straightforward, it is considerably more time consuming, and therefore the FFT approach is preferred.

3 Results

3.1 The dipole element

In this section we consider the thin dipole element, *i.e.*, dipole elements with small width compared to its length. The well known sine and cosine base commonly used for these elements [5] and the FEM current modes of the present approach are identical, see (2.4). Hence, the dipole element is a good element to consider when verifying the Fourier transform of the FEM current modes, since this Fourier transform can be expressed in closed form. In Figure 6 the transmission coefficient of a symmetric biplanar FSS structure, consisting of two slot arrays, is depicted. The slots are arranged in a square lattice, tilted 45°, with the side 17.25 mm. The two arrays are separated by a 7.0 mm thick loss-less dielectric spacer with the dielectric constant $\epsilon = 1.10$. Loss-less dielectric skins with the thickness 0.5 mm are located outside the slot arrays, see Figure 6. Three curves are depicted in the figure. The solid curve is computed by using ordinary cosine and sine basis functions [5], while the dashed curves are computed by the present FEM/FFT approach using a zero-padded FFT grid of 512×512 and 1024×1024 points, respectively. Three current modes are used and the two FEM/FFT approach curves are computed with an resolution of $N = 200$, see Figure 5. Moreover, $(2 \times 5 + 1)^2$ Floquet waves are

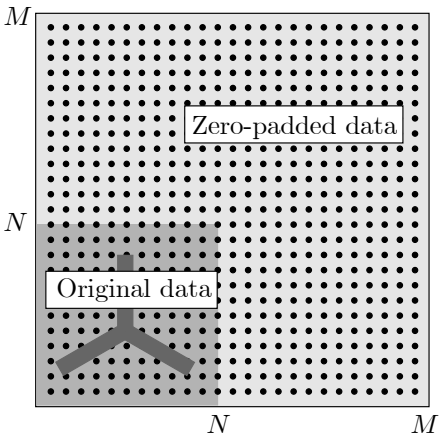

Figure 5: The technique of zero-padding is applied in order to increase the resolution in the spectral domain.

included. From the figure it is concluded that a zero-padded FFT grid of 512×512 points is not sufficient. However, it is found that 1024×1024 points are sufficient in general.

3.2 The three legged element

In this section we consider the tripole element, or in other words, the three legged element. We compute the transmission coefficient of an array of tripoles arranged in an equilateral lattice, see Figure 7. The transmission for this tripole array has been measured by other authors [16] for parallel polarization, and for the angles of incidence $\theta = 45°$ and $\phi = 90°$. Here, θ is measured from the normal of the FSS such that $\theta = 0°$ corresponds to normal incidence. Furthermore, the angle ϕ is measured from the x-axis toward the y-axis, see Figure 7.

We calculate the transmission according to Section 2 with 3 current modes, see Figure 2–4. Hence, the matrix in the linear system of equations, for the induced surface current, has the size 3×3. The effect of including more basis functions has been investigated, but no significant change of the results was found. However, if a larger frequency band is considered, *e.g.*, a frequency band including the second resonance, more basis functions have to be included in order to get adequate results. Moreover, 33^2 Floquet modes are included (truncation over a square). This truncation is determined by adding Floquet modes until the result does not change. The result is depicted in Figure 8.

3.3 The four legged element

As a third example we consider the four legged element, *i.e.*, the crossed dipole. From a computional point of view, this element is interesting to consider because there must be a connector mode supporting current flow from one arm to the other,

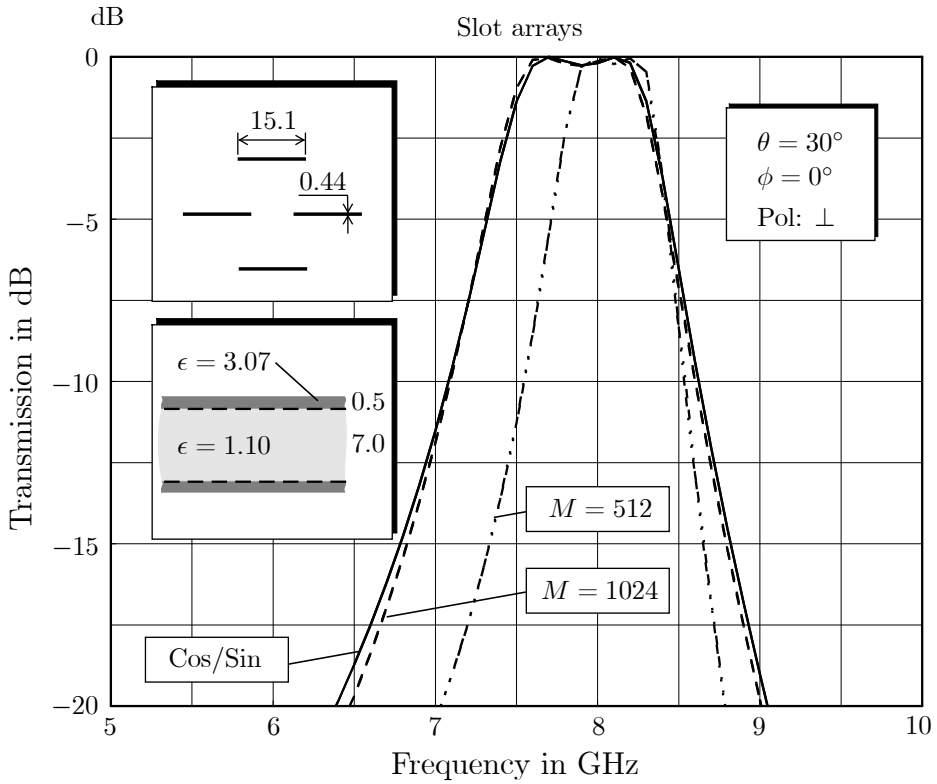

Figure 6: The transmission coefficient of a biplanar FSS structure. The slot elements are linear dipoles with the length 15.1 mm. Three curves are depicted in the figure. The solid curve is computed by using ordinary cosine and sine basis functions, while the dashed curves are computed by the present FEM/FFT approach using a zero-padded FFT grid of 512×512 and 1024×1024 points, respectively.

in order to approximate the current at the second resonance [9], denoted f_2 in Figure 9. It has also been shown that the standard sine and cosine functions yield extremely slow convergence of the solution [10]. We consider an array of crossed dipoles arranged in a square lattice, tilted 45°, with the side 17.25 mm. The length of the dipole arms is 15.1 mm, while the width is 0.44 mm. Pelton and Munk have reported measured results for this configuration [9]. Figure 9 depicts the reflection coefficient for parallel polarization. The angle of incidence is 60°.

4 Conclusions

In this paper waveguide modes obtained by the FEM were successfully used for surface current expansion in frequency selective surfaces. The commercial available code FlexPDE solved the Helmholtz' eigenvalue problem and saved a requested number of modes in text files. These current modes were then used in the MoM procedure in order to solve for the induced surface current, by means of the well known spectral Galerkin method [15]. It was found that for standard element geometries,

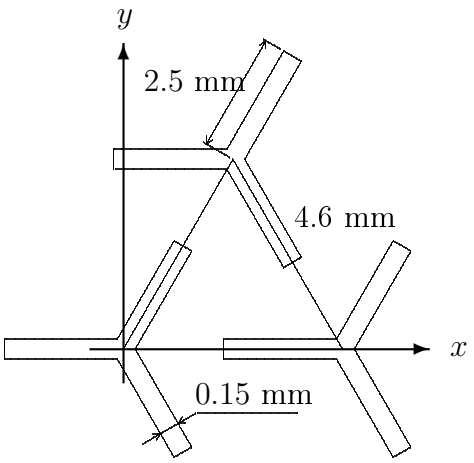

Figure 7: The equilateral triangular lattice. The length and width of the tripole arms are $L = 2.5$ and $W = 0.15$ mm, respectively.

e.g., the dipole, the FEM current modes were similar to the modes used by other authors. The FEM current modes have successfully been applied to a variety of FSS configurations, slot as well as dipole elements, and to both single and dual layer structures, including dielectric layers. The results have been compared to results obtained by the PMM and Oresme code, with excellent agreement.

References

[1] L. W. Henderson. *The scattering of planar arrays of arbitrarily shaped slot and/or wire elements in a stratified dielectric medium*. PhD thesis, Ohio State University, Department of Electrical Engineering, ElectroScience Laboratory, 1320 Kinnear Road, Columbus, Ohio 43212, USA, 1983.

[2] L. W. Henderson. Introduction to PMM, version 4.0. Technical Report 725347-1, ElectroScience Laboratory, Ohio State University, Department of Electrical Engineering, 1320 Kinnear Road, Columbus, Ohio 43212, USA, 1993.

[3] R. J. Langley and E. A. Parker. Equivalent circuit model for arrays of square loops. *Electronics Letters*, **18**(7), 294–296, 1982.

[4] N. Marcuvitz. *Waveguide Handbook*. McGraw-Hill, New York, 1951.

[5] R. Mittra, C. H. Chan, and T. Cwik. Techniques for analyzing frequency selective surfaces—A review. *Proc. IEEE*, **76**(12), 1593–1615, 1988.

[6] B. Munk. *Frequency Selective Surfaces: Theory and Design*. John Wiley & Sons, New York, 2000.

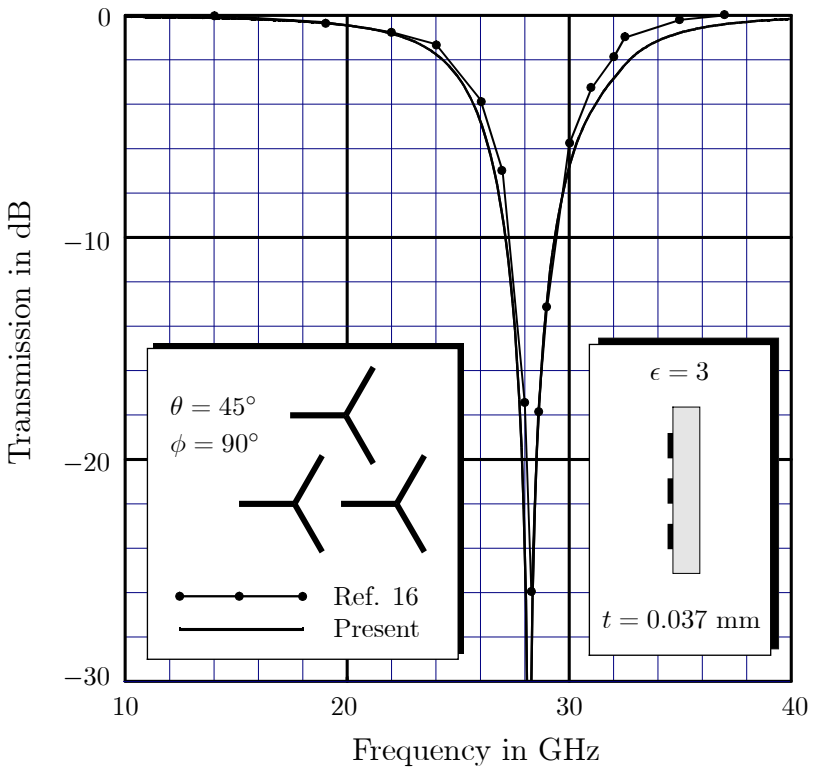

Figure 8: Predicted and measured transmission for parallel polarization.

[7] A. V. Oppenheim and R. W. Schafer. *Discrete-time signal processing.* Signal processing series. Prentice-Hall, Inc., 1999.

[8] E. A. Parker and S. M. A. Hamdy. Rings as elements for FSS. *Electronics Letters*, **17**(17), 612–614, August 1981.

[9] E. L. Pelton and B. A. Munk. Scattering from periodic arrays of crossed dipoles. *IEEE Trans. Antennas Propagat.*, **27**(3), 323–330, 1979.

[10] S. Poulsen. Scattering from frequency selective surfaces: A continuity condition for entire domain basis functions and an improved set of basis functions for crossed dipole. *IEE Proc.-H Microwaves, Antennas and Propagation*, **146**(3), 234–240, 1999.

[11] S. Poulsen. Scattering from frequency selective surfaces: An efficient set of V-dipole basis functions. *IEEE Trans. Antennas Propagat.*, **51**(3), 540–548, 2003.

[12] S. M. Rao, D. R. Wilton, and A. W. Glisson. Electromagnetic scattering by surfaces of arbitrary shape. *IEEE Trans. Antennas Propagat.*, **30**(3), 409–418, 1982.

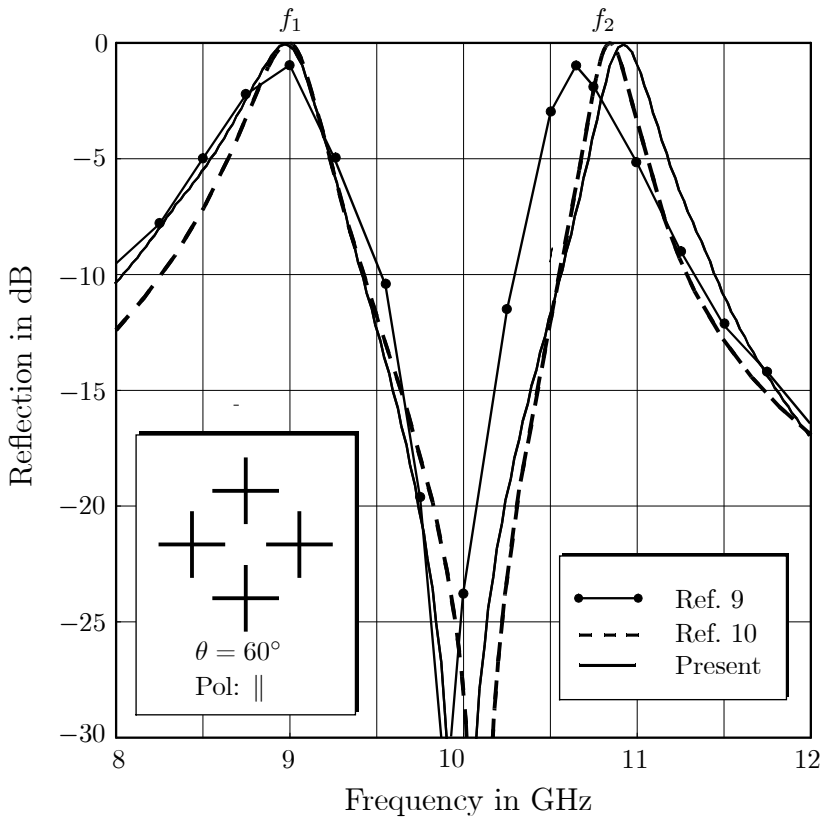

Figure 9: Reflection for the crossed dipole array.

[13] B. J. Rubin and H. L. Bertoni. Reflection from periodically perforated plane using subsectional current approximation. *IEEE Trans. Antennas Propagat.*, **31**(6), 829–836, November 1983.

[14] P. P. Silvester. Finite-element solution of homogeneous waveguide problems. *Alta Frequenza*, **38**, 313–317, 1969.

[15] C.-H. Tsao and R. Mittra. Spectral-domain analysis of frequency selective surfaces comprised of periodic arrays of cross dipoles and Jerusalem crosses. *IEEE Trans. Antennas Propagat.*, **32**(5), 478–486, 1984.

[16] J. C. Vardaxoglou and E. A. Parker. Performance of two tripole arrays as frequency-selective surfaces. *Electronics Letters*, **19**(18), 709–710, 1983.

Andrés Alayón Glazunov, Mats Gustafsson, Andreas F. Molisch, and Fredrik Tufvesson, "Physical Modeling of MIMO Antennas and Channels by Means of the Spherical Vector Wave Expansion," *LUTEDX/(TEAT-7177)/1-31/(2009).*

Andreas D. Ioannidis, Daniel Sjöberg, and Gerhard Kristensson, "On the propagation problem in a metallic homogeneous biisotropic waveguide," *LUTEDX/(TEAT-7178)/1-27/(2009).*

Anders Karlsson, Henrik Bladh, and Per-Erik Bengtsson, "An accurate method for predicting light scattering from soot aggregates with sub-particles of arbitrary shape and structure," *LUTEDX/(TEAT-7179)/1-22/(2009).*

Sven Nordebo, Andreas Fhager, Mats Gustafsson, Börje Nilsson, "Fisher information integral operator and spectral decomposition for inverse scattering problems," *LUTEDX/(TEAT-7180)/1-21/(2009).*

Mats Gustafsson, "Sum rule for the transmission cross section of apertures in thin opaque screens," *LUTEDX/(TEAT-7181)/1-8/(2009).*

Christer Larsson, Mats Gustafsson, and Gerhard Kristensson, "Wideband microwave measurements of the extinction cross section—Experimental techniques," *LUTEDX/(TEAT-7182)/1-22/(2009).*

Daniel Sjöberg and Mats Gustafsson, "Realization of a matching region between a radome and a ground plane," *LUTEDX/(TEAT-7183)/1-6/(2010).*

Kristin Persson, Mats Gustafsson, and Gerhard Kristensson, "Reconstruction and visualization of equivalent currents on a radome using an integral representation formulation," *LUTEDX/(TEAT-7184)/1-45/(2010).*

Mats Gustafsson, "Time-domain approach to the forward scattering sum rule," *LUTEDX/(TEAT-7185)/1-14/(2010).*

Mats Gustafsson and Daniel Sjöberg, "Sum rules and physical bounds on passive metamaterials," *LUTEDX/(TEAT-7186)/1-19/(2010).*

Mats Gustafsson, "Accurate and efficient evaluation of modal Green's functions," *LUTEDX/(TEAT-7187)/1-10/(2010).*

Alireza Kazemzadeh and Anders Karlsson, "Multilayered Wideband Absorbers for Oblique Angle of Incidence," *LUTEDX/(TEAT-7188)/1-18/(2010).*

Alireza Kazemzadeh and Anders Karlsson, "Nonmagnetic Ultra Wideband Absorber with Optimal Thickness," *LUTEDX/(TEAT-7189)/1-14/(2010).*

Daniel Sjöberg and Christer Larsson, "Cramér-Rao bounds for determination of permittivity and permeability in slabs," *LUTEDX/(TEAT-7190)/1-13/(2010).*

Anders Karlsson and Alireza Kazemzadeh, "On the Physical Limit of Radar Absorbers," *LUTEDX/(TEAT-7191)/1-10/(2010).*

Alireza Kazemzadeh, "Thin Wideband Absorber with Optimal Thickness," *LUTEDX/(TEAT-7192)/1-9/(2010).*

Anders Bernland, Annemarie Luger and Mats Gustafsson, "Sum Rules and Constraints on Passive Systems,"
LUTEDX/(TEAT-7193)/1-28/(2010).

Anders Bernland, Mats Gustafsson, and Sven Nordebo, "Physical Limitations on the Scattering of Electromagnetic Vector Spherical Waves,"
LUTEDX/(TEAT-7194)/1-23/(2010).

Mats Gustafsson, "Polarizability and physical bounds on antennas in cylindrical and rectangular geometries,"
LUTEDX/(TEAT-7195)/1-11/(2010).

Christer Larsson, Daniel Sjöberg, and Lisa Elmkvist, "Waveguide measurements of the permittivity and permeability at temperatures up to 1000 °C,"
LUTEDX/(TEAT-7196)/1-22/(2010).

Andreas Ioannidis, "On the cavity problem for the general linear medium in Electromagnetic Theory,"
LUTEDX/(TEAT-7197)/1-13/(2010).

Mats Gustafsson and Daniel Sjöberg, "Physical bounds and sum rules for high-impedance surfaces,"
LUTEDX/(TEAT-7198)/1-17/(2010).

Daniel Sjöberg, Mats Gustafsson, and Christer Larsson, "Physical bounds on the all-spectrum transmission through periodic arrays: oblique incidence,"
LUTEDX/(TEAT-7199)/1-13/(2010).

Mats Gustafsson, Marius Cismasu, and Sven Nordebo, "Absorption Efficiency and Physical Bounds on Antennas,"
LUTEDX/(TEAT-7200)/1-20/(2010).

Ruiyuan Tian, Buon Kiong Lau, and Zhinong Ying, "Characterization of MIMO Antennas with Multiplexing Efficiency,"
LUTEDX/(TEAT-7201)/1-6/(2010).

Andreas D. Ioannidis, Gerhard Kristensson, and Ioannis G. Stratis, "On the well-posedness of the Maxwell system for linear bianisotropic media,"
LUTEDX/(TEAT-7202)/1-25/(2010).

Gerhard Kristensson, "The polarizability and the capacity change of a bounded object in a parallel plate capacitor,"
LUTEDX/(TEAT-7203)/1-39/(2010).